

Reversible deactivation of higher-order posterior parietal areas. II. Alterations in response properties of neurons in areas 1 and 2

Adam B. Goldring, Dylan F. Cooke, Mary K. L. Baldwin, Gregg H. Recanzone, Adam G. Gordon, Tingrui Pan, Scott I. Simon and Leah Krubitzer

J Neurophysiol 112:2545-2560, 2014. First published 20 August 2014; doi:10.1152/jn.00141.2014

You might find this additional info useful...

This article cites 123 articles, 60 of which can be accessed free at:

</content/112/10/2545.full.html#ref-list-1>

Updated information and services including high resolution figures, can be found at:

</content/112/10/2545.full.html>

Additional material and information about *Journal of Neurophysiology* can be found at:

<http://www.the-aps.org/publications/jn>

This information is current as of December 5, 2014.

Reversible deactivation of higher-order posterior parietal areas. II. Alterations in response properties of neurons in areas 1 and 2

Adam B. Goldring,^{1,2*} Dylan F. Cooke,^{1,2*} Mary K. L. Baldwin,² Gregg H. Recanzone,^{2,3}
Adam G. Gordon,¹ Tingrui Pan,⁴ Scott I. Simon,⁴ and Leah Krubitzer^{1,2}

¹Center for Neuroscience, University of California, Davis, California; ²Department of Psychology, University of California, Davis, California; ³Department of Neurobiology, Physiology, and Behavior, University of California, Davis, California; and ⁴Department of Biomedical Engineering, University of California, Davis, California

Submitted 19 February 2014; accepted in final form 14 August 2014

Goldring AB, Cooke DF, Baldwin MK, Recanzone GH, Gordon AG, Pan T, Simon SI, Krubitzer L. Reversible deactivation of higher-order posterior parietal areas. II. Alterations in response properties of neurons in areas 1 and 2. *J Neurophysiol* 112: 2545–2560, 2014. First published August 20, 2014; doi:10.1152/jn.00141.2014.—The role that posterior parietal (PPC) and motor cortices play in modulating neural responses in somatosensory areas 1 and 2 was examined with reversible deactivation by transient cooling. Multiunit recordings from neurons in areas 1 and 2 were collected from six anesthetized adult monkeys (*Macaca mulatta*) before, during, and after reversible deactivation of areas 5L or 7b or motor cortex (M1/PM), while select locations on the hand and forelimb were stimulated. Response changes were quantified as increases and decreases to stimulus-driven activity relative to baseline and analyzed during three recording epochs: during deactivation (“cool”) and at two time points after deactivation (“rewarm 1,” “rewarm 2”). Although the type of response change observed was variable, for neurons at the recording sites tested >90% exhibited a significant change in response during cooling of 7b while cooling area 5L or M1/PM produced a change in 75% and 64% of sites, respectively. These results suggest that regions in the PPC, and to a lesser extent motor cortex, shape the response characteristics of neurons in areas 1 and 2 and that this kind of feedback modulation is necessary for normal somatosensory processing. Furthermore, this modulation appears to happen on a minute-by-minute basis and may serve as the substrate for phenomena such as somatosensory attention.

posterior parietal cortex; premotor cortex; motor cortex; cortical deactivation; feedback modulation

SOMATOSENSORY PROCESSING from the thalamus through the neocortex is characterized by both feedforward (e.g., Burton et al. 1995; Burton and Fabri 1995; Cusick et al. 1985; Darian-Smith et al. 1993; Gharbawie et al. 2010, 2011; Lewis and Van Essen 2000; Padberg et al. 2009; Pons and Kaas 1986; Rozzi et al. 2006) and feedback (Burton and Fabri 1995; Cavada and Goldman-Rakic 1989a, 1989b; Darian-Smith et al. 1999; Felleman and Van Essen 1991; Pons and Kaas 1986; Weber and Yin 1984; Yeterian and Pandya 1985) connections. The feedforward connections within cortex are fairly well understood: In both macaques and humans, receptive fields become larger and more complex as one moves between areas from anterior to posterior in the parietal lobe (Ashaber et al. 2014; Costanzo and Gardner 1980; Gardner 1988; Hyvärinen and Poranen

1978a, 1978b; Iwamura et al. 1980, 1983a, 1983b, 1985a, 1985b, 1994; Iwamura and Tanaka 1993; Nelson et al. 1980; Papadelis et al. 2011; Pei et al. 2010; Sanchez-Panchuelo et al. 2012; Sur 1980; Wacker et al. 2011; Yau et al. 2013), and ablation of “lower-order” areas such as 3a or 3b can abolish responses in more posterior areas such as area 1 (Garraghty et al. 1990). However, comparatively less is known about the function of feedback connections, especially in the somatosensory system. Studies of corticothalamic feedback in several species have demonstrated that deactivation of anterior parietal cortical areas can modulate the function of neurons in the somatosensory thalamus (see Cooke et al. 2014 for review). However, this phenomenon clearly does not extend to every branch of the somatosensory processing network, as studies in cats (Turman et al. 1995), marmosets (Zhang et al. 2001), and macaques (Pons et al. 1987) indicate that deactivating or ablating S2 has negligible effects on the response properties of neurons in various anterior parietal cortical areas. Beyond these few experiments focused on S2 modulation of anterior parietal neurons, relatively few studies have examined the role of corticocortical feedback modulation in the somatosensory system and none have examined the influence of posterior parietal cortex (PPC) on earlier stages of processing.

In the companion study, we found that cooling areas in PPC and motor cortex often resulted in changes to the size and location of receptive fields of neurons in areas 1 and 2. We also found that, on average, receptive fields of anterior parietal neurons expanded during cooling of 7b. We also observed that in some sites during the rewarm epochs (reactivation) the effect persisted or was enhanced (Cooke et al. 2014). The goal of that study was to stimulate the entire hand while recording from neurons in areas 1 or 2 in order to define the precise location and size of receptive fields with classical “best-area” hand-mapping techniques (e.g., Hyvärinen and Poranen 1978a; Iwamura et al. 1980; Kaas et al. 1979; Krubitzer et al. 2004; Nelson et al. 1980; Padberg et al. 2005, 2007; Pons et al. 1985; Seelke et al. 2012). However, while that investigation used a binary response measure (i.e., either in the best area or not) and could delineate receptive fields with fine spatial resolution, it did not allow us to quantify the subtle changes in response strength that can only be measured with automated stimuli. In that study, only extreme changes in response strength that concurrently altered the borders of a receptive field could be measured. More subtle, but potentially more numerous, changes may not have been large enough to meet the response criteria for that measure.

* A. B. Goldring and D. F. Cooke contributed equally to this work.

Address for reprint requests and other correspondence: L. Krubitzer, Center for Neuroscience, 1544 Newton Ct., Davis, CA 95618 (e-mail: lakrubitzer@ucdavis.edu).

In the present study we used automated stimuli to quantify the response strength and temporal dynamics of neurons in areas 1 and 2 during cooling of the same PPC and motor cortical areas. While the strengths of each technique (greater spatial resolution in defining changes in a receptive field vs. ability to quantify subtle changes in neural response) are complementary, differences in the type of stimuli used and type of analyses employed necessitate a separate consideration of the two data sets. In this study, we addressed three main questions: 1) Does deactivation of areas 5L and 7b and primary motor/premotor cortex (M1/PM) modulate the response of neurons in anterior parietal cortex (areas 1 and 2)? 2) Do the areas deactivated have differential effects on the neural response of areas 1 and 2? 3) Do these alterations in neural response persist beyond the immediate perturbation of the network?

MATERIALS AND METHODS

Six macaque monkeys (*Macaca mulatta*; 2 females, 4 males) were used to examine the effects of reversible deactivation of posterior parietal areas or motor cortex on the response properties of neurons in anterior parietal areas 1 and 2. In acute preparations, one to three small microfluidic thermal regulators (“cooling chips”) were surgically implanted onto the pial surface of areas 7b and 5L and/or on motor cortex (Fig. 1; Fig. 5 of Cooke et al. 2014). The design, fabrication, and cooling properties of these cooling chips have been discussed previously (Cooke et al. 2012). Since the time of that publication a newer design of cooling chip with a smaller cooling footprint has been implemented (see Cooke et al. 2014). Electrophysiological recordings of neural activity in areas 1 and 2 were collected prior to, during, and after cooling each region of interest. All surgical and experimental procedures were approved by the University of California, Davis Institutional Animal Care and Use Committee and followed guidelines published by the National Institutes of Health. Surgical procedures and chip implantation are described in Cooke et al. (2014).

Recording epochs. In the analyses of neural responses from each recording site in area 1 or 2 we designated three or four recording epochs based on the timing of cooling deactivation in areas 5L and 7b and M1/PM: 1) the “baseline” epoch was defined as the period prior to the onset of cooling deactivation; 2) the “cool” epoch was defined as the time after the region stabilized at the desired target temperature (20–25°C in cortex or 2°C at the chip-cortex interface), ~5–8 min after cooling was initiated; 3) the “rewarm 1” epoch was defined as 5–12 min after the cooled region returned to the baseline temperature following the cessation of cooling; and 4) the “rewarm 2” epoch was defined in three animals as the period following the rewarm 1 epoch, ~19–24 min after cooling ceased. This later epoch was used to assess whether the pattern of neuronal responses returned to baseline after an extended period of rewarming. Each epoch usually required 5–10 min to obtain a full set of data; thus testing at some sites, particularly those with a fourth recording epoch (rewarm 2), could last up to 90 min. A target temperature of 20–25°C in cortex was chosen for deactivation. Some reports suggest that cooling below this temperature is necessary to abolish all neural activity (Benita and Conde 1972), while numerous other studies have used this and warmer target temperatures to disrupt cortical activity (e.g., Chafee and Goldman-Rakic 2000; Girard et al. 1989; Lomber et al. 1999).

Electrophysiological recordings. Details of electrophysiological parameters and histological processing can be found in Cooke et al. (2014). Briefly, once the electrode was lowered to the appropriate depth, we quickly determined the strength of the response by grossly stimulating portions of the hand and forelimb. We quickly explored 270 sites to determine receptive field location, strength of response,

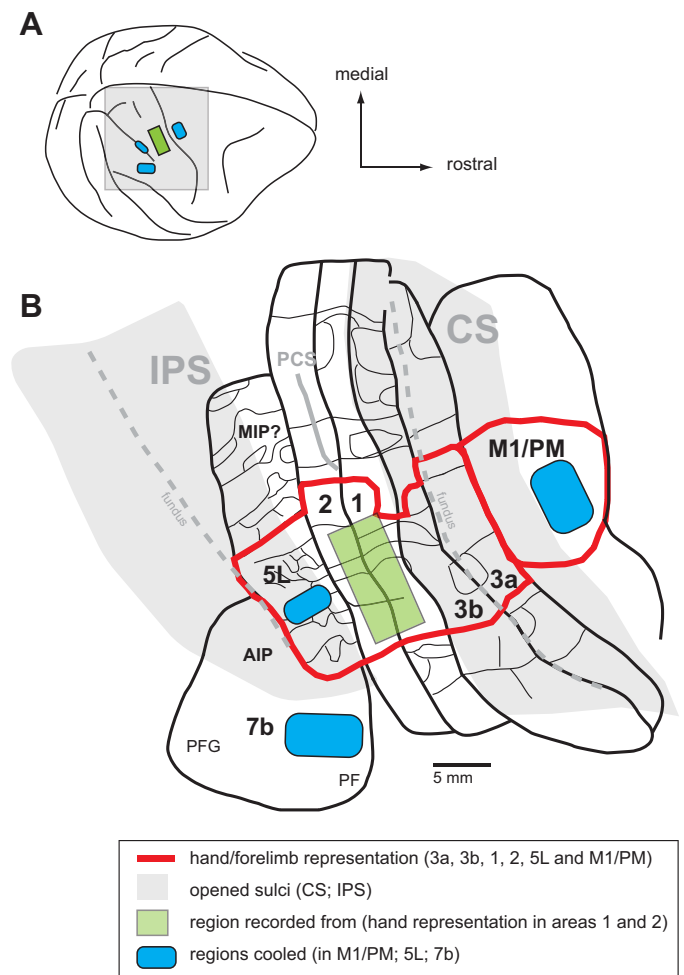


Fig. 1. A composite diagram of cooling chip placement relative to sulcal landmarks and cortical field maps. *A*: dorsolateral view of the monkey neocortex with the region of interest shaded gray. *B*: enlargement of the shaded region in *A* showing the location of areas 3a, 3b, 1, 2, M1/PM, 5L, and 7b (thick black lines) relative to each other and to the central sulcus (CS) and intraparietal sulcus (IPS). These sulci have been opened (gray shading) so that all cortical fields can be seen. Parietal areas 3a, 3b, 1, 2, and 5L have been mapped in detail in previous studies. Functional divisions between body part representations are shown in some fields (thin black lines); the hand representation in each area is outlined in red. Likewise, the location and organization of the motor hand representation have been identified in previous studies using microstimulation techniques. Note that the hand representation across these motor/parietal fields is consistently located at the same mediolateral level so that recordings in areas 3a, 1, and 2, as well as sulcal landmarks, allow for accurate placement of cooling chips in areas M1/PM and 5L. Area 7b has also been described in previous studies, and its location relative to the tip of the IPS has been well established. The blue shading indicates the locations of our cooling chips in the different monkeys: on the gyral surface of areas M1/PM and 7b and in the IPS in area 5. The green rectangle in areas 1 and 2 represents the location in the hand/forearm representation where electrophysiological recordings were made. This illustration has been modified from Seelke et al. (2012) with permission and also includes maps redrawn from Nelson et al. (1980) and Godschalk et al. (1995) with permission. See Table 3 for abbreviations.

and whether the neurons could be robustly driven by our stimulus. Of these 270 sites, only 58 sites were studied in detail and recorded during our cooling/rewarming epochs. For sites that were explored further, the receptive field was defined with standard hand mapping techniques, and computer-controlled tactile stimuli were placed in three or four locations within and outside the receptive field. If the computer-controlled stimuli could elicit a robust multiunit response

that was easy to separate from background activity when visualized on an oscilloscope, we recorded from that site during cooling of 5L, 7b, or M1. Here we report the neural responses to these suprathreshold tactile stimuli.

Stimulation paradigm. A computer-controlled system was used to stimulate the center of the receptive field plus three other locations on the hand or forelimb adjacent to the receptive field (Fig. 2). The stimulation system consisted of four adjustable hoses (Loc-Line, Lockwood Products, Lake Oswego, OR) each with a stainless steel nozzle (1.6- to 3.0-mm inner diameter, Stainless Steel Probe Point Cannula, Vita Needle, Needham, MA). A stream of pressurized air was controlled by a solenoid valve that was activated by a computer-controlled relay. When the valve was opened, the airstream passed through the adjustable hose and through the stainless steel nozzle. All four nozzles were coupled to the same manifold that connected to a common air tank. Since only one solenoid valve was open at a time, each nozzle received an equivalent volume of air under the same amount of pressure. All four nozzles were precisely aimed and secured (Fig. 2) such that a restricted portion of the hand or arm was stimulated consistently across all three or four recording epochs of the recording session for each recording site. In addition, the hand was secured with padded weights or attached to a custom-made adjustable frame with loose-fitting zip ties (Fig. 2). This prevented limb position from drifting over time. The adjustable frame was configured to hold the forelimb in postures that could be naturally maintained in the anesthetized animal and did not constrict blood flow.

Spike2 software controlled and recorded the timing and duration of air puffs through digital voltage output from the Power 1401 hardware to the solenoid relay. This allowed neuronal responses to be precisely aligned with the air-puff stimuli. Each location was stimulated with a 300-ms puff of air with a 700-ms interstimulus interval (for some sites, it was a 200-ms puff and an 800-ms interval). Each location was stimulated 15–30 times per epoch. In early cases (2/6), each location was stimulated with a separate block of air puffs during each recording epoch (i.e., *location A* 30 times during baseline, then *location B* 30 times during baseline, then *location A* during cool, then *location B* during cool, etc.), with no stimulation occurring between epochs. In later cases (4/6), stimulation locations were interleaved (i.e., *A, B, C, D, A, B, C, D...* for a total of 30 each) and stimulation took place both during and between recording epochs.

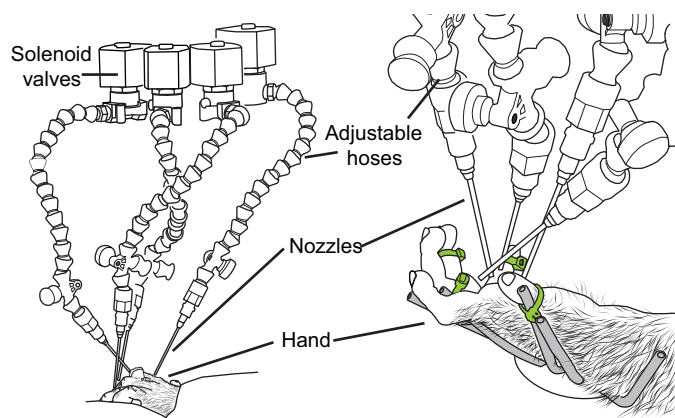


Fig. 2. Automated somatosensory stimulator directed at a monkey hand. *Left*: 4 computer-controlled solenoid valves positioned above the monkey's hand started and stopped a stream of pressurized air. Air from an open valve passed through an adjustable hose and nozzle precisely positioned to stimulate a restricted portion of the hand. *Right*: the hand was secured to a stationary frame (gray) with loosely fitting zip ties (green). Once in place, this stimulator setup remained stationary through all recording epochs (baseline, cool, rewarm 1, rewarm 2).

Computer-cued manual stimulation. The computer-controlled stimulation system described above provided light cutaneous stimulation to the glabrous skin of the hand or hairy skin of the hand and arm. However, at some sites (e.g., in area 2) neurons required more intense stimulation to activate deep receptors of the skin or joints. In these instances a stimulation location on the hand was marked with a permanent marker as a target for stimulation by a handheld von Frey hair. A custom Spike2 script produced and recorded the timing of a series of auditory tones that signaled to the experimenter when to stimulate the marked location. Each tone lasted 1,000 ms, with a 1,000-ms intertone interval. Each skin location was stimulated 15–30 times per epoch. Because of small errors in handheld stimulation timing relative to that of stimulus cues recorded in the data, neuronal responses could not be as precisely aligned to the actual timing of manual stimuli. For this reason a larger sampling window was employed in the subsequent analyses of data collected with this paradigm (see *Quantification of neural responses*).

Definition of neural responses. One of the goals of these experiments was to record from a sufficient number of sites per animal to appreciate any heterogeneity in response to cooling a given area. To achieve this goal, we made use of relatively low-impedance electrodes to record the activity of small clusters of neurons. This precluded the isolation of single units in the subsequent off-line analysis. Therefore, we quantified these neuronal responses as the neuronal activity that crossed a certain voltage amplitude (“trigger level”) determined by the mean and variance of the background activity preceding somatosensory stimulation. This process is illustrated in Fig. 3. To define this mean and variance, we analyzed the 300–500 ms of neuronal activity before the onset of the first stimulus (Fig. 3A). Figure 3B shows an expanded view of a small portion of this baseline activity. We then smoothed the waveform during this period by averaging the activity in a 0.1- to 0.5-ms window around each unit of time of the recorded activity (Fig. 3C). We chose the smallest window that allowed for reliable peak and trough detection (see below) during each recording epoch for each site. Typical widths and amplitudes of the smoothed peaks and troughs of activity were identified by the experimenter and used as parameters to detect peaks and troughs of this averaged background activity with Spike2's “Peak and Trough Find” active cursor mode, which is represented in Fig. 3B as arrows. These peaks and troughs were then used to center sampling windows over the raw waveform (Fig. 3B). At each peak or trough in the smoothed waveform, the maximum or minimum voltage was recorded from the raw waveform within a sampling window equal to the peak or trough width at its base. The maxima and minima of the peaks and troughs of the raw waveform were independently used to calculate the mean and variance of the positive or negative amplitude of background activity. The polarity of the trigger level for a given site was set by the direction in which stimulus-driven responses had the greatest value, relative to baseline. For example, if the negative component of stimulus-evoked spikes was of smaller width and greater in amplitude than the positive-going component (as in Fig. 3D), the negative trigger level was used to detect multiunit events for that epoch. A sampling window was set around each trigger-crossing such that only one multiunit event would be recorded within 0.8 ms of a trigger-crossing (Fig. 3E). Trigger levels were set at the mean positive or negative amplitude of background activity plus or minus 5 or 6 standard deviations (Fig. 3A; higher trigger values were chosen when the signal was difficult to distinguish from background noise). Throughout these experiments, we often observed changes in background activity and signal-to-noise ratios during different recording epochs. Therefore, to ensure that trigger levels within each site were based on a consistent number of standard deviations above or below the mean background activity, trigger levels were set independently for each recording epoch based on corresponding background activity. However, the polarity of the trigger level was consistent across epochs.

Quantification of neural responses. Peristimulus time histograms showed that before, during, and after cooling a large proportion (and

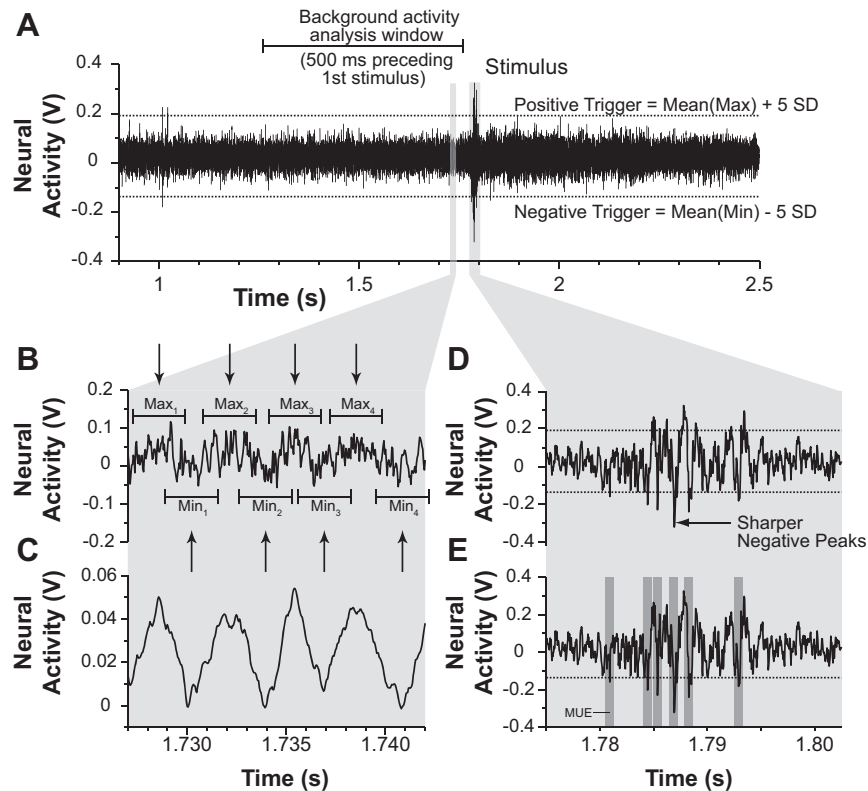


Fig. 3. Illustration depicting how stimulus-driven neural responses were quantified. *A*: the 500 ms preceding the first automated stimulus was analyzed in order to calculate the mean and SD of background activity. The window of time analyzed is shown as the areas within the bracket above the voltage trace. *B*: expanded view of 15 ms within the analysis window. The raw neural activity can be seen as an oscillating waveform with noise and background activity superimposed over it. The goal was to find the mean and SD of the positive (peaks) component and the negative component (troughs) of the noise. *C*: to detect the peaks and troughs automatically, the raw trace was smoothed with a 0.1- to 0.5-ms window. This allowed for automatic peak and trough detection (black arrows) that could be aligned to the raw activity trace (shown in *B*). Maxima and minima of the peaks and troughs of the raw activity trace were collected by centering a sampling window over the peaks and troughs of the smoothed trace and sampling from the raw trace. The mean maxima and minima were used to calculate positive and negative trigger levels (shown in *A*) for detection of multiunit events. *D*: expanded view of stimulus-driven activity shown in *A*. The polarity of the chosen trigger level was determined by visualizing which component of the spikes (positive or negative) had the highest amplitude and thinnest width. In this example, the negative components of the spikes peaked more sharply (arrow) and at higher amplitude than the positive components, so a negative trigger level is chosen. *E*: multiunit events were defined as any crossing of the chosen trigger level/polarity. Only 1 multiunit event (MUE) was counted in a 0.8-ms window (dark gray shading) centered on the trigger crossing. Trigger levels were calculated independently for each recording epoch. However, the polarity of the trigger levels remained constant for the entire deactivation test.

often nearly all) of the neuronal response occurred within 80 ms of stimulus onset. Therefore, we restricted our analysis of the response to this window of time (0–80 ms) to compare the neuronal response during different recording epochs to the baseline warm epoch. This analysis window would allow us to measure the firing rate during each epoch even if cooling induced a latency difference in the “on” response (a phenomenon that we did not observe). For each trial, the firing rate was calculated within this driven-response window as well as during a spontaneous activity window of equal length immediately prior to stimulation onset. For sites in which computer-cued manual stimulation was used, the width of the stimulus-driven analysis window was increased to 200 ms before and after the onset of the auditory cue. The corresponding spontaneous activity window was defined as the 400 ms preceding the stimulus-driven analysis.

Statistical analysis. The difference between driven and spontaneous activity was used to compare activity across recording epochs. The distribution of this difference was often nonnormal and varied across different recording epochs, as did the variance. We therefore analyzed the differences in the mean response during each recording epoch with a two-sample bootstrap test for unequal variances (Good 2005). For this procedure, bootstrap samples of our difference measure were drawn at random within each recording epoch until each epoch’s sample was equal to the number of trials within that epoch. The difference in mean response between the two recording epochs

was then calculated. This procedure was repeated 5,000 times to construct a distribution of differences in response between the two recording epochs. If the 97.5% confidence interval of this distribution (2-tailed test) did not contain the difference of 0, then the mean response of the two recording epochs was deemed significantly different. Each later recording epoch was compared to the baseline (precooling) period in this manner.

To compare the types and magnitude of changes evoked by cooling each region of interest (M1/PM, 7b, or 5L) we categorized the change in response of the area 1/2 neurons between the baseline and the other recording epochs into one of four categories (see *Population analysis*, Fig. 8). Recording sites in areas 1 and 2 were categorized as “only increase in response” if the only significant change(s) was increase in response to stimulation of one or more locations on the hand or forelimb; “only decrease in response” if the only significant change(s) was a decreased response; “mix” if both increased and decreased responses were observed during stimulation of different portions of the hand or forelimb; and “no change” for no significant changes. The proportion of recording sites exhibiting one of these categories of change was compared with the Freeman-Halton extension of Fisher’s exact test. For each later recording epoch, four separate 2×3 (type of change \times cooled area) contingency tables were constructed to compare the proportion of sites showing a given type of change (e.g., “only increase”) relative to all other possible changes (i.e., “only

Table 1. Cases: deactivation tests by regions cooled

Case	Area Cooled (mm ²)	Deactivation Tests	
		Response change/total	% Changed
11-186	5L (21.0)	7/9	77.7
12-12	5L (6.7)	5/6	83.3
	7b (39.3)	5/7	71.4
	M1 (22.2)	3/5	60.0
	Total 13/18		72.2
12-59	7b (9.6)	19/21	90.5
	M1 (24.3)	1/3	33.3
	Total 20/24		83.3
12-100	7b (6.8)	1/1	100
	M1 (4.6)	2/2	100
	Total 3/3		100
12-149	5L (13.7)	6/8	75.0
	7b (6.8)	6/6	100
	M1 (6.8)	3/4	75.0
	Total 15/18		83.3
12-150	7b (6.8)	8/8	100
Total across 6 cases			
	5L	18/23	78.3
	7b	39/43	90.7
	M1	9/14	64.3
Total for all cases, all cooling locations			
		66/80	82.5

Area cooled is surface area of cooling footprint on cortex. Sites with “changed” response are defined as those with any statistically significant change in the neuronal response to stimulation at 1 or more sites on the hand during the cold epoch. Up to 3 deactivation tests (cooling of areas 5L, 7b, and M1) could be conducted at a single recording site; therefore the deactivation test totals here are often greater than the totals for recording sites examined with cooling in Table 2 (e.g., grand totals of 80 and 58, respectively).

decrease,” “mix,” or “no change”) during or after the cooling of each area (M1/PM, 7b, or 5L).

RESULTS

Of the 270 recording sites in six monkeys, 58 sites were examined in detail because neurons at these sites could be driven discretely by stimulation of at least one location by our tactile stimuli. Some sites were tested during cooling of multiple, successive areas; hence the sum of such “deactivation tests” (80, see Table 1) is more than the number of sites tested (58, see Table 2). Table 1 shows the numbers of deactivation tests studied during cooling, broken down by case, field cooled, and the proportion of sites at which we observed changes in neuronal responses during cooling. Of these, 31 recording sites were in area 1, 10 were in area 2, and 17 were located on the border between the two areas (see Table 2). The preponderance of responses to cutaneous stimulation suggests that most of the sites located on the border between areas 1 and 2 were actually in area 1. Fisher’s exact test revealed no significant relationship between the area recorded from (i.e., area 1, area 2, or the border) and the type of response changes observed during cooling (increase, decrease, or mixed, $P = 0.29$; see MATERIALS AND METHODS). Consequently, data from all recording sites have been combined in subsequent analyses, and we use the term “area 1/2” to define their location. Responses of each site were tested before, during, and after cooling of one or more neighboring fields including areas 5L and 7b and M1/PM. Tables 1 and 2 show the numbers of sites studied in each case and the number of sites studied during cooling of different fields.

Representative single-site examples. Figure 4 is a representative example of the multiunit response of area 1/2 neurons to stimulation of several locations on the glabrous surface of the hand before, during, and after cooling of area 5L. As can be seen from the rasters as well as the mean difference in firing rate during the baseline epoch, the magnitude of the responses of the neurons at this representative site differed depending on the location on the hand that was stimulated. The strongest response is shown in Fig. 4A and the weakest in Fig. 4C. Cooling area 5L resulted in a statistically significant decrease in the response of these area 1/2 neurons to stimulation across all locations on the hand. Interestingly, although cooling elicited a decrease in response at each stimulation location, the response to stimulation upon rewarming 5L was anisometric across locations. While the response of these neurons to stimulation of the locations in Fig. 4, A and B, returned to baseline upon rewarming of area 5L, the response to stimulation of the locations shown in Fig. 4, C and D, was significantly lower than baseline. In fact, cooling of area 5L abolished the response to stimulation of the location in Fig. 4C entirely.

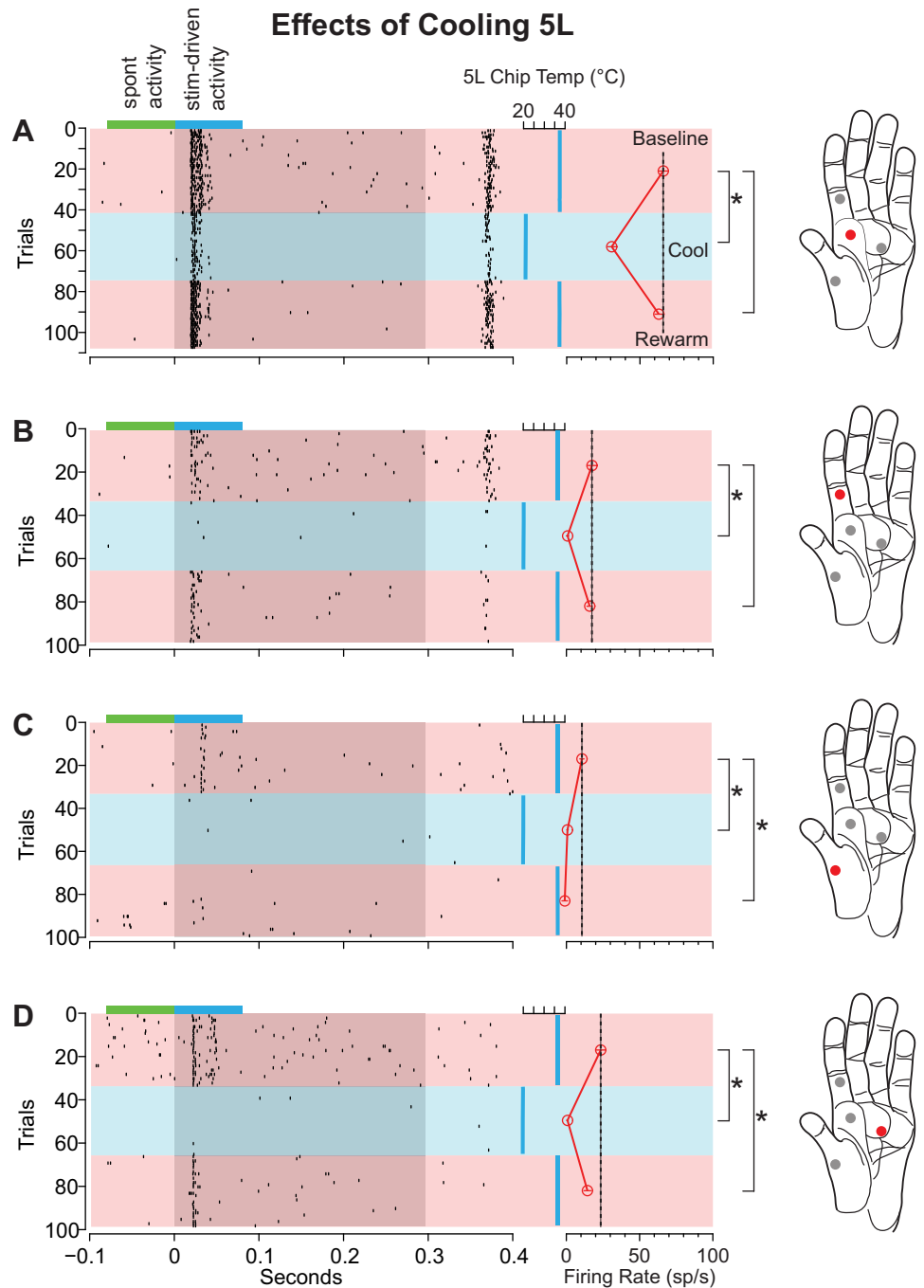
The multiunit response of a typical cluster of area 1/2 neurons to stimulation of several locations on the glabrous surface of the hand before, during, and after cooling of M1/PM is depicted in Fig. 5. Note that in addition to testing during an additional recording epoch (rewarm 2) data were collected between epochs for this and later cases. As in the previous example for cooling area 5L (Fig. 4), the initial response to stimulation at each location differed, with the location shown in Fig. 5B eliciting the strongest response and the location shown in Fig. 5D the weakest. In contrast to the previous example, cooling M1/PM to 20°C gradually increased the response of the neurons within the site and produced a statistically significant increase at all stimulation locations. As in the previous example, although cooling elicited an increase in response at each stimulation location, the response to stimulation upon rewarming M1/PM was anisometric across locations. While the response to stimulation of locations in Fig. 5, A and D, returned to baseline immediately, stimulation of the locations in Fig. 5, B and C, produced a significantly greater response during the rewarm 1 epoch compared with baseline. Furthermore, the response to stimulation of the location shown in Fig. 5C did not return to baseline during the rewarm 2 epoch (14 min after the cessation of cooling).

At some sites, cooling produced an increase in response to stimulation at some locations while producing a decrease in response at others. Figure 6 illustrates this effect during cooling of area 7b. While stimulation of the location in Fig. 6D elicited the strongest response at baseline, cooling produced a

Table 2. Cases: recording sites

Case	Recording Sites (sites examined with cooling/total sites)			
	Area 1	1/2 Border	Area 2	Total
11-186	7/33	1/9	1/9	9/51
12-12	6/15	1/6	0/6	7/27
12-59	9/30	8/21	6/40	23/91
12-100	0/0	3/9	0/21	3/30
12-149	4/24	1/13	3/17	8/57
12-150	5/10	3/7	0/0	8/17
Total across 6 cases	31/112	17/65	10/93	58/270

Fig. 4. Differential changes in the neural responses of area 1/2 neurons during cooling of area 5L in case 11-186. This example illustrates a decrease in firing rate with cooling for all 4 stimulation sites on the hand and, for locations C and D, a persistent effect. Locations on the glabrous surface of the monkey's hand (right) that were stimulated in succession with the 4-way air puffer illustrated in Fig. 3 are shown as red and gray circles. Neuronal response to the stimulation of a given location on the hand (red circle) is shown in the panel on left of each hand (A–D). Each dot in the raster (left) represents 1 multiunit event. Gray region denotes the duration of the air-puff stimulus (~300 ms). Cortical temperature is plotted as a vertical blue line on right of gray region. Different temperature analysis epochs are denoted by different color horizontal bars (pink, baseline; blue, cool; pink, rewarm). For each trial, the spontaneous firing rate (sp/s) was calculated and subtracted from the stimulus-driven firing rate. This difference in firing rate was used to calculate a mean difference in firing rate for each recording epoch (red open circles connected by red vertical line). The mean and SE (thin red lines within open circles) of each epoch are shown on right of the temperature trace. Black vertical dashed line marks the mean difference in firing rate for stimulus-driven activity for the baseline epoch (top pink horizontal bar). This dashed line spans all recording epochs to facilitate comparisons between the baseline neuronal firing rate with the firing rate for cool and rewarm epochs. Small blue horizontal bar at the top of each raster denotes the analysis window for stimulus-driven activity. Adjacent green bar denotes the window for spontaneous activity. Brackets with asterisks (on left of each hand) indicate a significant difference in firing relative to the baseline epoch (97.5% bootstrapped confidence interval). Cooling area 5L produced a marked decrease in the response of area 1/2 neurons to stimulation at all locations tested. However, while the neuronal response to stimulation of locations A and B returned to baseline after warming, the response to stimulation of locations C and D did not.



significant decrease in neuronal response while simultaneously evoking an increase in neuronal response to stimulation of the locations shown in Fig. 6, A and B. With respect to the “cool” epoch, this site would be categorized as exhibiting a “mixed” response (see *Population analysis*, Fig. 8).

Occasionally, the strength and placement of our automated stimulus allowed us to study changes in the hand-mapped receptive fields as well as the strength of response to the air-puff stimuli. Figure 7 illustrates such a situation during cooling of area 7b. Diagrams of the dorsal surface of the hand in Fig. 7, right, show not only the location being stimulated by the air puffer but also the extent of the hand-mapped receptive field during each recording epoch. The baseline receptive field

was mapped prior to stimulation. The extent of the receptive field was then remapped immediately after stimulation in each subsequent epoch. The baseline hand-mapped receptive field shows a strong response to stimulation of the distal and middle portion of D2 and the entirety of D3 on the dorsal surface. We placed two of the air puffers within the hand-mapped baseline receptive field and two outside the hand-mapped receptive field. Stimulation of locations shown in Fig. 7, A and B (corresponding to the middle of dorsal D1 and D2, respectively), with the air-puff stimulus elicits a strong response, while stimulation of locations shown in Fig. 7, C and D (outside of the hand-mapped receptive field) elicits a negligible response. Upon cooling 7b, the hand-mapped receptive field

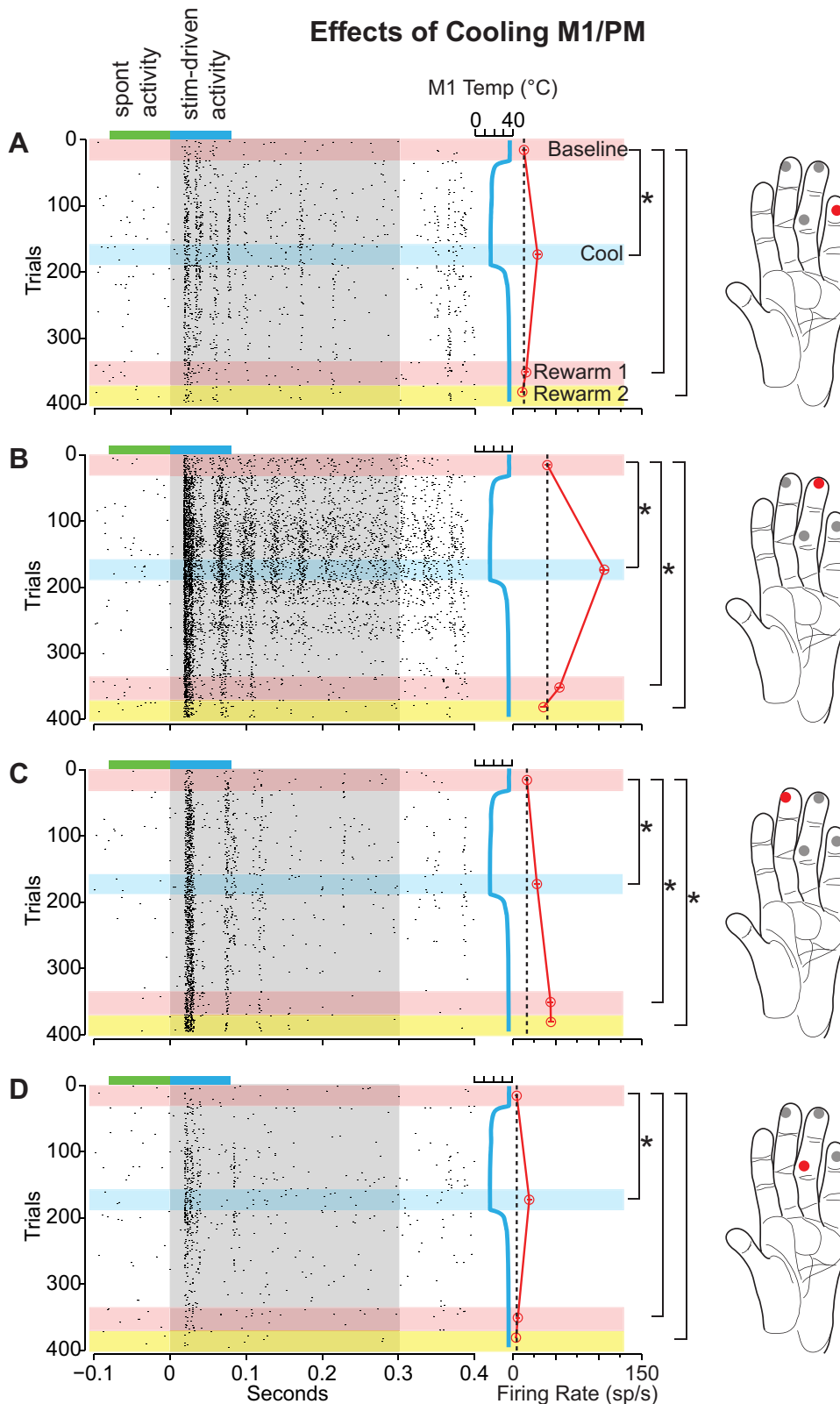


Fig. 5. Differential changes in the neural responses of area 1/2 neurons during cooling of M1/PM for case 12-149. Presentation of stimuli at different locations was interleaved (see *Stimulation paradigm*). This example illustrates an increase in firing rate with cooling for all 4 stimulation sites on the hand and, for *location C*, a persistent and enhanced effect. While cooling produced a significant increase in response at each stimulation location, only *locations A, B, and D* returned to a baseline level of responsiveness after warming. Conventions are the same as Fig. 4 (except that the pink horizontal bar indicates the rewarm 1 epoch and the yellow horizontal bar indicates the rewarm 2 epoch).

expands to include the middle and part of the distal phalange of dorsal D4. This expansion of the receptive field can be seen as the emergence of a new response to stimulation in Fig. 7C with our automated stimulus. A significant increase in firing rate was observed in response both to stimulation of this location

and to stimulation of the locations shown in Fig. 7, A and B. During the rewarm epoch, the mean and standard deviation of spontaneous activity increased by 17% and 93%, respectively, raising the trigger level relative to previous epochs. Thus no multiunit events were able to reach the trigger level, and the

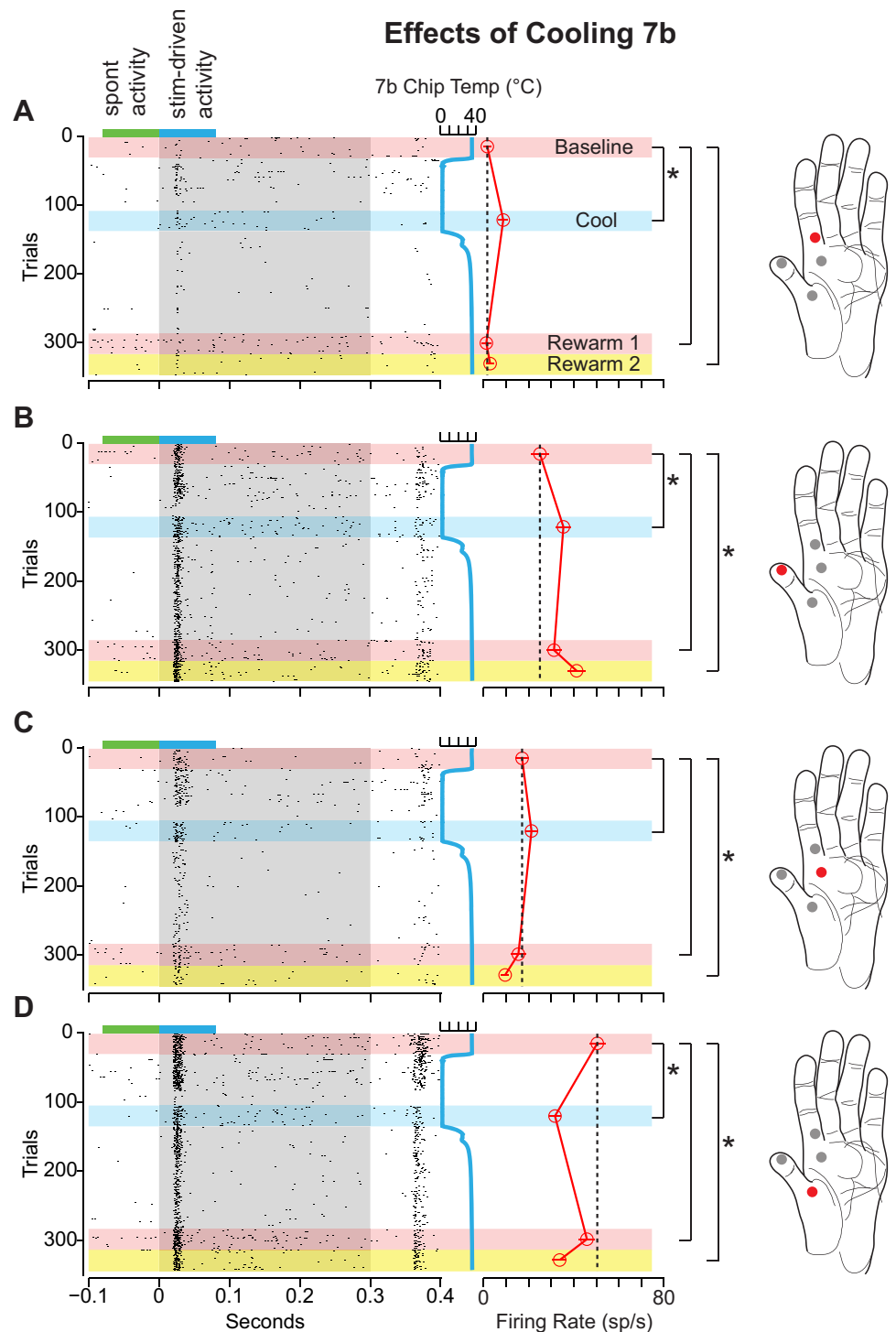


Fig. 6. Example of a mixed response to different stimulation locations on the hand during cooling of area 7b for case 12-150. Presentation of stimuli at different locations was interleaved (as in Fig. 5). Stimulation of location D elicited the strongest response from area 1/2 neurons at baseline. Cooling area 7b significantly reduced the neuronal response to stimulation at location D. However, the opposite effect was observed during stimulation of locations A and B. With regard to both the cool and rewarm 2 epochs, this site would be categorized as showing a “mixed” pattern in the subsequent population analysis (see Fig. 8).

mean activity during this epoch dropped regardless of stimulation site. Despite this increase in background activity, responses to our hand-mapping stimuli could still be determined unambiguously, and the expansion of the receptive field was recorded as persisting into this epoch.

Population analysis. When the data from individual sites were considered together, several patterns emerged that revealed the likelihood of observing a given type of change in firing rate of area 1/2 neurons during and after the cooling of each area. For these analyses, we were interested in how

cooling or rewarming different cortical areas modulated the magnitude of the responses of neurons in area 1/2. Figure 8 illustrates the proportion of sites exhibiting the four different patterns of change based on the response magnitude organized by recording epoch. Although a majority of neurons showed some kind of change, especially when cooling areas 5 and 7b, overall the pattern of changes evoked by cooling any region was quite variable. Similarly variable patterns were observed in the subsequent rewarm 1 (Fig. 8, center) and rewarm 2 (Fig. 8, right) epochs. The variability in response change, correc-

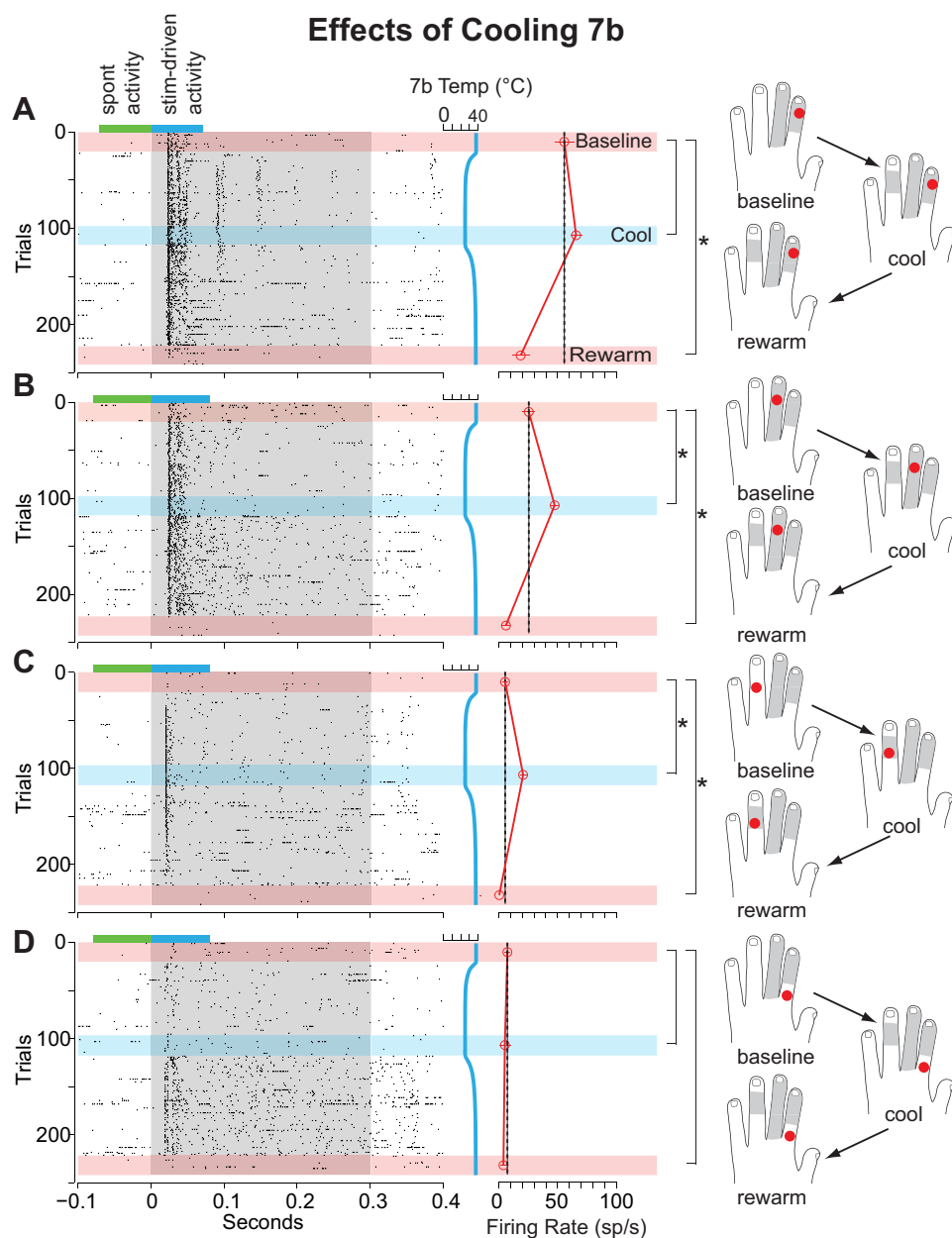


Fig. 7. Example of the differential changes in the neural responses of area 1/2 neurons during cooling of area 7b in case 12-59 coregistered with the hand mapping data. Gray shaded region on each model hand denotes the extent of the hand-mapped receptive field during each recording epoch. At baseline, stimulation of *locations A* and *B* elicited a neural response, while stimulation at *locations C* and *D* had a negligible response. Cooling produced a significant increase in the response of area 1/2 neurons to stimulation at *site B*, and a previously unseen response emerged by stimulating *site C* during cooling. Conventions are the same as in Figs. 4 and 5.

tions for multiple post hoc comparisons, and the relatively low number of sites tested during cooling of M1 likely contribute to the fact that Fisher's exact test did not reveal any significant relationship between the area cooled or rewarmed and a given type of response change. Similarly, only a small proportion of sites were tested during the rewarm 2 epoch, making it difficult to draw conclusions about the longevity of any persistent changes and the magnitude of effect of this epoch compared with others. Nonetheless, the population analysis of response strength has revealed a general pattern: Reducing the activity from posterior parietal and motor areas most frequently resulted in a decrease in the activity of area 1/2 neurons during this inactivation. Furthermore, some of these changes persisted once cooling had ceased and some emerged de novo during this time.

Taken together, our results demonstrate that cooling and rewarming posterior parietal and motor areas modulated the

activity of area 1 and 2 neurons in a heterogeneous manner with regard to both the location of stimulus presentation on the hand (i.e., receptive field configuration) and the amplitude and sign of neuronal response. This variability of modulation combined with the lack of a priori knowledge about the type of modulation we expected precluded the observation of a significant relationship between the area cooled and the type of modulation observed. Nonetheless, we consistently observed response modulation of anterior parietal neurons as a result of altering the activity of neurons in areas 5L and 7b and to a lesser extent M1/PM.

DISCUSSION

Hierarchical serial processing and somatosensory feedback. Areas within PPC contain neurons with complex receptive fields that are heavily modulated by attention, behavioral

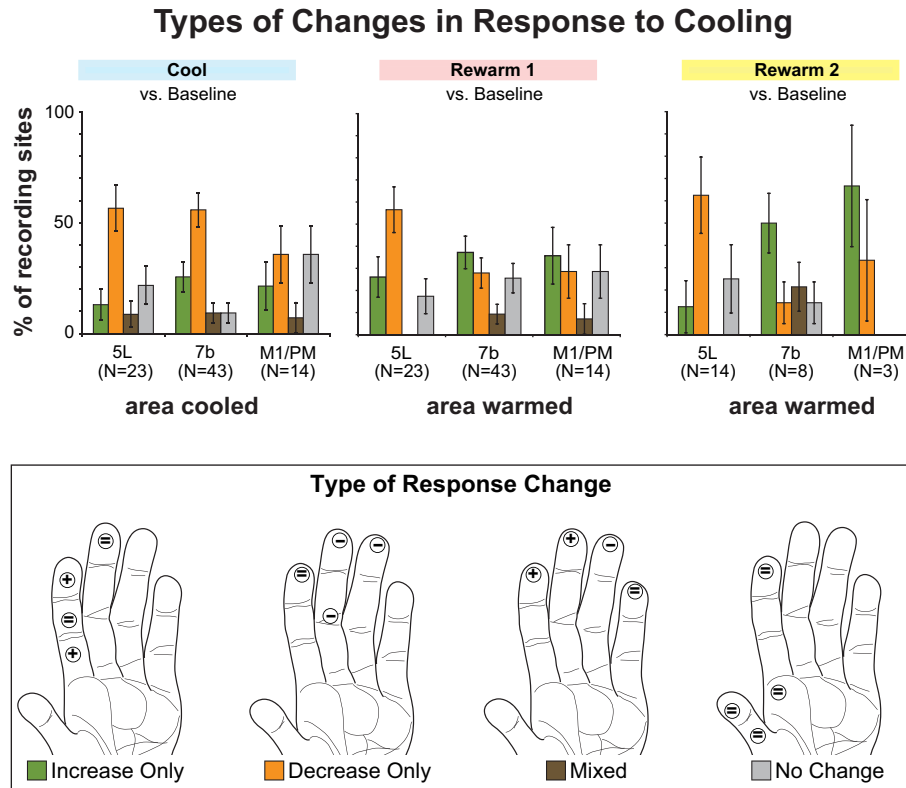


Fig. 8. Proportion of recording sites displaying different types of activity changes (color coded in key and graphically represented on a diagram of the hand) in response to cooling and rewarming areas 5L or 7b or M1/PM. For each recording epoch (*top*) % of sites showing 1 of 4 activity patterns was calculated. Error bars = SE. “Increase Only” (green): cooling or rewarming induced a significant ($P < 0.025$, 2-tailed test) increase in the neuronal response to stimulation of 1 or more of the 4 locations on the hand that were stimulated. The hand depicted (*bottom*) illustrates the response to cooling area 7b at recording site 5 in case 12-150. The response to stimulation increases at 2 locations (plus signs) but remains unchanged at the other 2 (equal signs). “Decrease Only” (orange): same definition as above, but for significant decreases in neuronal response. The hand illustrates the response to cooling area 5L at site 2 in case 12-149. The response to stimulation decreases at 3 locations (minus signs) but remains unchanged at the 4th. “Mixed” (brown): cooling or rewarming induced a decrease in response to stimulation for at least 1 location and an increase in response at 1 or more other stimulation locations. The hand illustrates the response to cooling area 5L at site 33 from case 11-186. Two locations show an increase in response to stimulation, 1 shows a decrease, and the 4th remains unchanged. “No Change” (gray): cooling or warming did not induce any significant changes in neuronal response to stimulation of any tested stimulation locations on the hand. The hand illustrates the response to cooling M1/PM at site 31 from case 12-149. None of the locations shows any change in response to stimulation during compared with baseline.

context, and motor planning (Batista and Andersen 2001; Baumann et al. 2009; Bisley and Goldberg 2003; Buschman and Miller 2007; Cui and Andersen 2007; Gail and Andersen 2006; Ipata et al. 2006; Lynch et al. 1977; Mountcastle et al. 1975). Specifically, area 5L in macaques contains neurons with large receptive fields located exclusively on the shoulder, arm, and hand that often span multiple digits/joints and occasionally have bilateral receptive fields (Duffy and Burchfiel 1971; Iwamura et al. 1994, 2002; Seelke et al. 2012). In addition, neurons in this subdivision of area 5 are responsive when a monkey engages in reaching and grasping behavior, with the peak of activity occurring during the early stages of prehension before an object is grasped (Chen et al. 2009; Gardner et al. 2007a, 2007b). Area 7b in macaque monkeys is comprised of neurons with large, directionally selective somatosensory receptive fields representing the arm, hand, and face; nociceptive and thermoceptive neurons; and neurons with visual receptive fields focused on peripersonal space, three-dimensional object selectivity, and responses to multimodal stimulation (Dong et al. 1994; Hyvärinen 1981; Hyvärinen and Poranen 1974;

Leinonen et al. 1979; Leinonen and Nyman 1979; Rozzi et al. 2008). While Brodmann’s area 7b has since been subdivided into multiple divisions, including PF and PFG (see Table 3 for abbreviations) (Gregoriou et al. 2006; Rozzi et al. 2006, 2008), our cooling devices likely covered portions of both subdivisions. Rozzi et al. (2008) demonstrated that PFG contains a higher proportion of visually responsive neurons than PF, with most neurons tuned to object presentation in peripersonal space; mirror neurons were also observed. That same study found that PF contains a substantially larger proportion of neurons responsive to somatosensory stimulation. While nearly all of PF’s somatosensory neurons responded to orofacial stimulation, PFG had similar proportions of neurons responsive to stimulation of the face/mouth, hand, and arm. Both areas 5L and 7b receive dense projections from anterior parietal cortical areas (Burton and Fabri 1995; Cavada and Goldman-Rakic 1989a; Gharbawie et al. 2011; Lewis and Van Essen 2000; Rozzi et al. 2006) that share overlapping connections from thalamic nuclei characterized by a large amount of convergence and divergence (Kasdon and Jacobson 1978;

Table 3. *Abbreviations*

<i>Body parts</i>	
D1–5	Digits 1–5
P1–3	Palmar pads 1–3
<i>Cortical fields and structures</i>	
1	Area 1; cutaneous representation caudal to area 3b
2	Area 2; representation of deep receptors caudal to area 1
3b	Area 3b, primary somatosensory area, S1 proper
5L	Area 5, lateral division (as defined in Seelke et al. 2012)
7b	Area 7b; posterior parietal area on the lateral operculum
AIP	Anterior intraparietal area
CS	Central sulcus
IPS	Intraparietal sulcus
M1	Primary motor cortex
MIP	Medial intraparietal area
PCS	Post central sulcus
PF	Parietal area F, overlaps 7b
PFG	Parietal area FG, overlaps 7b
PM	Premotor cortex

Padberg et al. 2009; Pons and Kaas 1985; Schmammann and Pandya 1990; Weber and Yin 1984). It is thought that both these converging corticocortical and thalamocortical connections give rise to the complex response properties observed in PPC neurons. It has also been known for some time that the anatomical substrate for feedback modulation of anterior parietal neurons is present in the form of direct and indirect feedback connections (Burton and Fabri 1995; Cavada and Goldman-Rakic 1989a, 1989b; Cooke et al. 2014; Felleman and Van Essen 1991; Pons and Kaas 1986; Rozzi et al. 2006; Weber and Yin 1984; Yeterian and Pandya 1985). However, comparatively little attention has been paid to what kind of influence these “higher-order” posterior parietal areas might have on cortical areas involved in early sensory processing.

To our knowledge, the only study that examined the effects of PPC manipulation on neurons in anterior parietal cortex was conducted by Padberg et al. (2010), who characterized receptive fields of neurons in areas 1 and 2 before and after a discrete lesion was made to area 5L. Within 60 min of the lesion, receptive fields of neurons within areas 1 and 2 exhibited a variety of changes including expansions, contractions, and locational shifts on the hand and forelimb. In that study, a larger proportion of sites exhibited receptive field changes following lesions compared with the companion paper to the present study, in which cooling was employed (Cooke et al. 2014). Several factors could account for this difference including the time of remapping (5 min after inactivation vs. 60 min after lesion), differences in the congruency between chip vs. lesion placement, and general differences between aspiration lesions and thermal deactivation. While the study of Padberg et al. (2010) did not quantify changes in anterior parietal neuronal response strength following 5L lesions, the results are largely congruent with the present investigation and its companion study: Deactivation of area 5L can alter receptive field size and location of neurons within areas 1 and 2. We extend this study by demonstrating the temporal dynamics of this phenomenon and quantifying alterations in neural response. In addition, we demonstrate similar findings for a separate posterior parietal area, 7b.

Although deactivating motor cortex did not modulate the response strength of anterior parietal neurons as consistently as deactivation of PPC areas, it still resulted in modulation more often than not. Consistent with our results, cooling of the forelimb region of motor cortex in macaques has been shown to modulate the cortical field potentials of homotypical locations in postcentral somatosensory cortex during a lever-lifting task (Sasaki and Gemba 1984). Recent work in rats has demonstrated that inactivation of motor cortex via muscimol disrupts anticipatory firing patterns in S1 that precede an active whisking task (Pais-Vieira et al. 2013). Similarly, Lee et al. (2013) have demonstrated that chemical inactivation of vibrissal M1 in mice uncouples the activity of disinhibitory vasointestinal peptide (VIP) interneurons in S1 from active whisking behavior. Zhang et al. (2013) have also demonstrated a pattern of local field potential synchrony between S1 and primary vibrissal motor cortex (vM1) during passive whisker movement and active whisking. They further showed that chemical inactivation of vM1 slowed whisking-related rhythms in S1 while optogenetic stimulation of vM1 increased S1 multiunit activity. Similar work in macaques (London and Miller 2013) and humans (Cui et al. 2014) has shown that differential activity in area 2 during active vs. passive movements may be due to efference copies of motor signals from M1. This suggests that modulation of somatosensory function by motor cortex may be a shared trait among mammals, rather than a specialization unique to primates.

An important observation in the present investigation regarding the temporal dynamics of deactivations of posterior parietal fields and motor cortex is that in 76% of the recording sites neurons did not return to their baseline activity (rewarm epochs). In our companion study (Cooke et al. 2014) we also demonstrated that receptive fields in 35% of recording sites did not return to their original size or configuration after cooling and rewarming. While it is possible that in those sites that showed a persistent decrease in activity some cells may have died or were no longer isolated, the presence of multiunits that showed a persistent increase in activity suggests that this cannot be the case for all sites. In our companion paper we discuss the possibility that persistent effects observed during the rewarm epochs are due to longer-latency and possibly irreversible alterations in the efficacy of synapses within that cortical network, alterations that may occur under natural conditions at a local level across the cortical sheet. In essence, cooling has changed activity in the areas recorded and possibly elsewhere in the somatosensory network, which in turn changed synaptic efficacy throughout the network as well (for further discussion, see Cooke et al. 2014).

It is also possible that had we waited longer than 24 min neurons would have reverted back to baseline level, since some studies indicate that neurons may require as long as 30 min to an hour of rewarming to return to baseline (Alexander and Fuster 1973; Girard et al. 1989, 1991, 1992; Huang et al. 2007). However, if this is not the case, then our data set is likely comprised of a mixture of neurons in area 1/2 that show varying degrees of reversibility. While many studies that employ cooling only show select examples of rewarm activity relative to baseline, changes either persisting into or arising de novo during the rewarm epoch are common (e.g., Carrasco and Lomber 2009, 2010; Clemo and Stein 1986; Girardin and Martin 2009; Michalski et al. 1993; Murray et al. 1992; Ponce

et al. 2008, 2011; Turman et al. 1992; Zhang and Murray 1996). Furthermore, slice preparations of hippocampal (Aihara et al. 2001) and cortical (Volgushev et al. 2004) tissue have demonstrated that rewarming neural tissue after cooling can lower the threshold for spike generation, increase the number of spikes elicited by current injection, and increase the probability of neurotransmitter release compared with baseline. These changes likely underpin the “rebound” activity seen in our study and others during rewarming but do not explain why changes persist.

Comparisons with receptive field changes during cooling. In our companion investigation we used the same cooling techniques to deactivate areas 5L and 7b and M1/PM while documenting the changes in the size and shape of somatosensory receptive fields of neurons in areas 1 and 2 with classic hand-mapping techniques (Cooke et al. 2014). While the methods employed in the present investigation had the advantage of being able to detect subtle changes in stimulus-driven activity, the advantage of the methods employed in the companion investigation was the ability to stimulate the entire hand with a high degree of spatial resolution. In that study, we found changes in the size and/or shape of receptive fields in neurons in areas 1 and 2, with most changes occurring when cooling and warming areas 7b and 5L. As in the present investigation, the changes in receptive fields were reversible at many but not all recording sites. Despite these similarities, there were several important differences in the methodologies. Cooke and colleagues sampled responses while stimulating many points on the hand, using classic hand-mapping techniques to document the full extent of the receptive field for neurons at a particular site. In contrast, here we examined four fixed points on the hand with our air-puff stimuli. When placing our stimulators, we had no knowledge about how the size and shape of a receptive field might change when cooling or warming a given region. Therefore, beyond the one or two stimulators placed inside the hand-mapped receptive field, the additional stimulators were directed at points adjacent to the hand-mapped receptive field, with the hope that these locations might capture the changes. Sometimes we did capture this change, but many times we did not (as determined via the hand-mapped receptive fields in the companion study).

Beyond this, the hand-mapped receptive field does not map directly onto the responses elicited by our air-puff stimuli for two important reasons. First, hand-mapped receptive fields were determined based on the strongest responses assessed by listening to them through a loudspeaker and observing them on an oscilloscope. In contrast, here we quantified the response to our air-puff stimulus via the average difference between spontaneous and stimulus-driven multiunit events during each recording epoch. Statistically significant changes in this difference measure might not be detected with our hand-mapping protocol. In the simplest of cases, an increase in neuronal response to air-puff stimulation inside the hand-mapped receptive field would not translate into any change in the receptive field's extent. Even a small but statistically significant decrease in activity in response to air-puff stimulation within the hand-mapped receptive field would not necessarily be of a large enough effect size to say that neurons were unresponsive while stimulating that portion of the hand. Similarly, a small but statistically significant increase in neuronal response to air-puff stimulation outside the hand-mapped receptive field would not

necessarily be large enough for inclusion in the receptive field with hand-mapping techniques.

A second issue that arises when comparing the methodology of this pair of studies is that the hand-mapped receptive fields were assessed by near-threshold stimulation with probes, brushes, and von Frey hairs. In contrast, our goal in positioning our air-puff stimulators was to elicit a robust response that could be easily quantified during off-line analysis. Therefore, our air-puff stimuli were usually suprathreshold and usually stimulated a larger portion of skin, which may have engaged both the center and the inhibitory surround of the receptive fields of neurons in areas 1 and 2 or evoked in-field inhibition (Gardner and Costanzo 1980; Hyvärinen and Poranen 1978a; Phillips et al. 1988; Sripathi et al. 2006; Sur 1980). These in-field and surround effects, combined with higher-amplitude stimuli, may be responsible for some of the differences in neuronal responses evoked by the air-puff stimuli compared with the stimulation used in the companion study. Regardless, as shown in Fig. 4D of Cooke et al. (2014), the response to the air-puff stimulus is generally consistent with the hand-mapped receptive field boundaries: Stimulation inside the receptive field elicits a much stronger response than stimulation of a nearby spot on the hand.

Taken together, differences in both the quantification of response and the quality of the stimuli are likely responsible for the lack of exact congruency in the details of the global measures in the two studies. The higher amplitude of our air-puff stimuli likely stimulated more of the hand and different receptor types and activated a greater number of neurons in areas 1 and 2. The combined lateral interactions of more neurons as well as the more complex responses elicited from activating center-surround and in-field inhibitory mechanisms may have resulted in our stimuli engaging a more heterogeneous set of feedback projections from PPC and motor cortex. Thus silencing feedback through deactivation may have resulted in a more varied response profile. Indeed, while the preponderance of decreases in activity may have been due to disfacilitation (i.e., loss of tonic excitation) seen during similar experiments in S2 (Turman et al. 1995; Zhang et al. 2001), heterogeneity in response changes seems to be a common phenomenon in experiments where feedback modulation is studied with reversible deactivation of higher-order fields (e.g., Alexander and Fuster 1973; Chafee and Goldman-Rakic 2000; Huang et al. 2007; Jansen-Amorim et al. 2011; Nassi et al. 2013).

Despite differences in the data sets of this study and the companion study, a clear picture has emerged from both studies: Altering the activity of areas 5L and 7b and to a lesser extent M1/PM frequently modulates the activity and increases the receptive field size of neurons in areas 1 and 2, a change that can persist even once the cortex has been rewarmed. In our companion paper, we propose that receptive field changes are due to disinhibition of inputs, particularly from area 7b (Cooke et al. 2014). However, the patterns of response changes observed in this investigation suggest that our automated stimuli may have engaged a more heterogeneous set of mechanisms, including a removal of tonic facilitation.

The role of feedback: attentional modulation? What is the purpose of this feedback modulation? It is possible that reversible deactivation of PPC/M1 may have simply disrupted a dynamic equilibrium of excitation and inhibition between neu-

rons in the areas cooled, in areas 1 and 2, as well as other areas of the network. However, it is also possible that our manipulation draws on a process of dynamic feedback that operates in awake animals during the execution of behaviors requiring selective attention to somatosensory stimuli. Several studies in both humans and macaques have demonstrated that the activity of anterior parietal cortical neurons is modulated by the demands of different behavioral tasks. Much like the visual system, this modulation in response is often interpreted as a top-down attentional mechanism to aid in the detection and discrimination of behaviorally salient stimuli. Braun and colleagues (2002) have shown that, in humans, directing attention to one finger vs. the entire hand can induce changes in the somatotopy of the hand representation within “S1” while performing a direction discrimination task. Goltz et al. (2013) have demonstrated that attending to a vibrotactile stimulus in anticipation of rare frequencies can increase the BOLD response across the entirety of human “S1” and “S2.” A growing body of work has also shown that directed attention to somatosensory stimuli can modulate oscillatory activity of “S1” in humans (Anderson and Ding 2011; Bardouille et al. 2010; Dockstader et al. 2010; Jones et al. 2010). Furthermore, selective attention to tactile stimulation of the hand has been shown to induce both decreases (Burton and Sinclair 2000; Hsiao et al. 1993) and increases (Ageranioti-Belanger and Chapman 1992; Chapman and Ageranioti-Belanger 1991; Chapman and Meftah 2005; Hyvärinen et al. 1980; Meftah et al. 2002) in the neuronal response of anterior parietal neurons in macaque monkeys. This type of attentional modulation is even more pronounced in S2, in terms of both frequency and strength (Burton et al. 1997; Chapman and Meftah 2005; Hsiao et al. 1993; Meftah et al. 2002). While there were some differences in these studies, all generally agreed that neurons in areas 1 and 2 are more consistently modulated than those in area 3b and that, regardless of the sign of modulation, this phenomenon aids in the detection and discrimination of task-relevant stimuli (Burton et al. 1997, 1999; Burton and Sinclair 2000; Hsiao et al. 1993; Hyvärinen et al. 1980; Meftah et al. 2002; Spingath et al. 2011, 2013; Wang et al. 2012).

Since we did not isolate single neurons in these studies, it is impossible to say whether the response changes we observed were due to the neurons we recorded at baseline changing their response strength, recruitment of previously silent neurons, or both. Despite this, specific hypotheses can be tested based on our results. One prediction would be that tactile discrimination ability and texture perception should be disrupted after reversible deactivation of areas 5L and 7b, and to a lesser extent motor cortex, because of the changes in the receptive field and neuronal responsiveness documented in this study and the companion study. Our laboratory is currently examining in awake monkeys the behavioral deficits evoked by cooling these same areas during several manual tasks and comparing them to deficits evoked by cooling regions in anterior parietal cortex, such as area 2 (Cooke et al. 2011). Another prediction would be that reversible deactivation of these posterior parietal and motor cortices may disrupt the modulation of area 1 and 2 neuronal responses evoked by selective attention.

This study and its companion (Cooke et al. 2014) provide some of the first evidence that the PPC can modulate the receptive field geometry and response strength of neurons in areas 1 and 2 in macaque monkeys. This suggests that somato-

sensory cortex in macaque monkeys is a highly dynamic network in which feedback, local circuits, and even interhemispheric connections dramatically modulate neuronal responses at multiple levels of processing. This kind of flexibility in somatosensory processing serves to gate, retain, or refine somatosensory inputs in order to select appropriate motor actions for a highly dynamic social context in which subtle visual, tactile, and auditory cues are constantly in flux.

ACKNOWLEDGMENTS

We thank Conor Weatherford, Arnold Chen, Syed Hussain, and Hoang Nguyen for assistance with data collection and analysis.

GRANTS

This work was supported by National Institutes of Health Grants R01 NS-035103 and R21 EB-012866 to L. Krubitzer and Vision Training Grant T32 EY-015387 to A. B. Goldring and M. K. L. Baldwin.

DISCLOSURES

No conflicts of interest, financial or otherwise, are declared by the author(s).

AUTHOR CONTRIBUTIONS

Author contributions: A.B.G., D.F.C., G.H.R., and L.K. conception and design of research; A.B.G., D.F.C., M.K.L.B., G.H.R., and L.K. performed experiments; A.B.G., D.F.C., M.K.L.B., and A.G.G. analyzed data; A.B.G., D.F.C., G.H.R., and L.K. interpreted results of experiments; A.B.G., D.F.C., M.K.L.B., and L.K. prepared figures; A.B.G., D.F.C., and L.K. drafted manuscript; A.B.G., D.F.C., M.K.L.B., G.H.R., A.G.G., T.P., S.I.S., and L.K. edited and revised manuscript; A.B.G., D.F.C., and L.K. approved final version of manuscript.

REFERENCES

- Ageranioti-Belanger S, Chapman C. Discharge properties of neurones in the hand area of primary somatosensory cortex in monkeys in relation to the performance of an active tactile discrimination task. *Exp Brain Res* 91: 207–228, 1992.
- Aihara H, Okada Y, Tamaki N. The effects of cooling and rewarming on the neuronal activity of pyramidal neurons in guinea pig hippocampal slices. *Brain Res* 893: 36–45, 2001.
- Alexander G, Fuster J. Effects of cooling prefrontal cortex on cell firing in the nucleus medialis dorsalis. *Brain Res* 61: 93–105, 1973.
- Anderson KL, Ding M. Attentional modulation of the somatosensory mu rhythm. *Neuroscience* 180: 165–180, 2011.
- Ashaber M, Pálfi E, Friedman RM, Palmer C, Jáklí B, Chen LM, Kántor O, Roe AW, Négyessy L. Connectivity of somatosensory cortical area 1 forms an anatomical substrate for the emergence of multifinger receptive fields and complex feature selectivity in the squirrel monkey (*Saimiri sciureus*). *J Comp Neurol* 522: 1769–1785, 2014.
- Bardouille T, Picton TW, Ross B. Attention modulates beta oscillations during prolonged tactile stimulation. *Eur J Neurosci* 31: 761–769, 2010.
- Batista A, Andersen R. The parietal reach region codes the next planned movement in a sequential reach task. *J Neurophysiol* 85: 539–544, 2001.
- Baumann MA, Fluett MC, Scherberger H. Context-specific grasp movement representation in the macaque anterior intraparietal area. *J Neurosci* 29: 6436–6448, 2009.
- Benita M, Conde H. Effects of local cooling upon conduction and synaptic transmission. *Brain Res* 62: 133–151, 1972.
- Bisley JW, Goldberg ME. Neuronal activity in the lateral intraparietal area and spatial attention. *Science* 299: 81–86, 2003.
- Braun C, Haug M, Wiech K, Birbaumer N, Elbert T, Roberts LE. Functional organization of primary somatosensory cortex depends on the focus of attention. *Neuroimage* 17: 1451–1458, 2002.
- Burton H, Abend NS, MacLeod AM, Sinclair RJ, Snyder AZ, Raichle ME. Tactile attention tasks enhance activation in somatosensory regions of parietal cortex: a positron emission tomography study. *Cereb Cortex* 9: 662–674, 1999.

- Burton H, Fabri M.** Ipsilateral intracortical connections of physiologically defined cutaneous representations in areas 3b and 1 of macaque monkeys: projections in the vicinity of the central sulcus. *J Comp Neurol* 355: 508–538, 1995.
- Burton H, Fabri M, Alloway K.** Cortical areas within the lateral sulcus connected to cutaneous representations in areas 3b and 1: a revised interpretation of the second somatosensory area in macaque monkeys. *J Comp Neurol* 355: 539–562, 1995.
- Burton H, Sinclair RJ.** Tactile-spatial and cross-modal attention effects in the primary somatosensory cortical areas 3b and 1–2 of rhesus monkeys. *Somatosens Motor Res* 17: 213–228, 2000.
- Burton H, Sinclair RJ, Hong SY, Pruett JR, Whang KC.** Tactile-spatial and cross-modal attention effects in the second somatosensory and 7b cortical areas of rhesus monkeys. *Somatosens Motor Res* 14: 237–267, 1997.
- Buschman TJ, Miller EK.** Top-down versus bottom-up control of attention in the prefrontal and posterior parietal cortices. *Science* 315: 1860–1862, 2007.
- Carrasco A, Lomber SG.** Evidence for hierarchical processing in cat auditory cortex: nonreciprocal influence of primary auditory cortex on the posterior auditory field. *J Neurosci* 29: 14323–14333, 2009.
- Carrasco A, Lomber SG.** Reciprocal modulatory influences between tonotopic and nontotopic cortical fields in the cat. *J Neurosci* 30: 1476–1487, 2010.
- Cavada C, Goldman-Rakic PS.** Posterior parietal cortex in rhesus monkey. I. Parcellation of areas based on distinctive limbic and sensory corticocortical connections. *J Comp Neurol* 287: 393–421, 1989a.
- Cavada C, Goldman-Rakic PS.** Posterior parietal cortex in rhesus monkey. II. Evidence for segregated corticocortical networks linking sensory and limbic areas with the frontal lobe. *J Comp Neurol* 287: 422–445, 1989b.
- Chafee M, Goldman-Rakic P.** Inactivation of parietal and prefrontal cortex reveals interdependence of neural activity during memory-guided saccades. *J Neurophysiol* 83: 1550–1566, 2000.
- Chapman C, Ageranioti-Belanger S.** Discharge properties of neurones in the hand area of primary somatosensory cortex in monkeys in relation to the performance of an active tactile discrimination task. *Exp Brain Res* 97: 319–339, 1991.
- Chapman CE, Meftah EM.** Independent controls of attentional influences in primary and secondary somatosensory cortex. *J Neurophysiol* 94: 4094–4107, 2005.
- Chen J, Reitzen SD, Kohlenstein JB, Gardner EP.** Neural representation of hand kinematics during prehension in posterior parietal cortex of the macaque monkey. *J Neurophysiol* 102: 3310–3328, 2009.
- Clemons HR, Stein BE.** Effects of cooling somatosensory cortex on response properties of tactile cells in the superior colliculus. *J Neurophysiol* 55: 1352–1368, 1986.
- Cooke DF, Goldring AB, Baldwin MK, Recanzone GH, Chen A, Pan T, Simon SI, Krubitzer L.** Reversible deactivation of higher-order posterior parietal areas. I. Alterations of receptive field characteristics in early stages of neocortical processing. *J Neurophysiol* (August 20, 2014). doi:10.1152/jn.00140.2014.
- Cooke DF, Goldring AB, Weatherford CB, Yamayoshi I, Recanzone GH, Simon SI, Krubitzer L.** Reversible brain deactivation by focal cooling in an awake behaving monkey: effects of deactivation of area 2, area 5, and area 7b on unimanual and bimanual reaching tasks (Abstract). *2011 Neuroscience Meeting Planner*. Program No. 82.02, 2011.
- Cooke DF, Goldring AB, Yamayoshi I, Tsourkas P, Recanzone GH, Tiriac A, Pan T, Simon SI, Krubitzer L.** Fabrication of an inexpensive, implantable cooling device for reversible brain deactivation in animals ranging from rodents to primates. *J Neurophysiol* 107: 3543–3558, 2012.
- Costanzo RM, Gardner EP.** A quantitative analysis of responses of direction-sensitive neurons in somatosensory cortex of awake monkeys. *J Neurophysiol* 43: 1319–1341, 1980.
- Cui F, Arnstein D, Thomas RM, Maurits NM, Keyzers C, Gazzola V.** Functional magnetic resonance imaging connectivity analyses reveal efference-copy to primary somatosensory area, BA2. *PLoS One* 9: e84367, 2014.
- Cui H, Andersen R.** Posterior parietal cortex encodes autonomously selected motor plans. *Neuron* 56: 552–559, 2007.
- Cusick CG, Steindler DA, Kaas JH.** Corticocortical and collateral thalamocortical connections of postcentral somatosensory cortical areas in squirrel monkeys: a double-labeling study with radiolabeled wheatgerm agglutinin and wheatgerm agglutinin conjugated to horseradish peroxidase. *Somatosens Res* 3: 1–31, 1985.
- Darian-Smith C, Darian-Smith I, Burman K, Ratcliffe N.** Ipsilateral cortical projections to areas 3a, 3b, and 4 in the macaque monkey. *J Comp Neurol* 335: 200–213, 1993.
- Darian-Smith C, Tan A, Edwards S.** Comparing thalamocortical and corticothalamic microstructure and spatial reciprocity in the macaque ventral posterolateral nucleus (VPLc) and medial pulvinar. *J Comp Neurol* 410: 211–234, 1999.
- Dockstader C, Cheyne D, Tannock R.** Cortical dynamics of selective attention to somatosensory events. *Neuroimage* 49: 1777–1785, 2010.
- Dong WK, Chudler EH, Sugiyama K, Roberts VJ, Hayashi T.** Somatosensory, multisensory, and task-related neurons in cortical area 7b (PF) of unanesthetized monkeys. *J Neurophysiol* 72: 542–564, 1994.
- Duffy F, Burchfiel J.** Somatosensory system: organizational hierarchy from single units in monkey area 5. *Science* 172: 273–275, 1971.
- Felleman DJ, Van Essen DC.** Distributed hierarchical processing in the primate cerebral cortex. *Cereb Cortex* 1: 1–47, 1991.
- Gail A, Andersen R.** Neural dynamics in monkey parietal reach region reflect context-specific sensorimotor transformations. *J Neurosci* 26: 9376–9384, 2006.
- Gardner E.** Somatosensory cortical mechanisms of feature detection in tactile and kinesthetic discrimination. *Can J Physiol Pharmacol* 66: 439–454, 1988.
- Gardner EP, Babu KS, Reitzen SD, Ghosh S, Brown AS, Chen J, Hall AL, Herzlinger MD, Kohlenstein JB, Ro JY.** Neurophysiology of prehension. I. Posterior parietal cortex and object-oriented hand behaviors. *J Neurophysiol* 97: 387–406, 2007a.
- Gardner EP, Costanzo RM.** Temporal integration of multiple-point stimuli in primary somatosensory cortical receptive fields of alert monkeys. *J Neurophysiol* 43: 444–468, 1980.
- Gardner EP, Ro JY, Babu KS, Ghosh S.** Neurophysiology of prehension. II. Response diversity in primary somatosensory (S-I) and motor (M-I) cortices. *J Neurophysiol* 97: 1656–1670, 2007b.
- Garraghty PE, Florence SL, Kaas JH.** Ablations of areas 3a and 3b of monkey somatosensory cortex abolish cutaneous responsiveness in area 1. *Brain Res* 528: 165–169, 1990.
- Gharbawie OA, Stepniewska I, Burish MJ, Kaas JH.** Thalamocortical connections of functional zones in posterior parietal cortex and frontal cortex motor regions in New World monkeys. *Cereb Cortex* 20: 2391–2410, 2010.
- Gharbawie OA, Stepniewska I, Kaas JH.** Cortical connections of functional zones in posterior parietal cortex and frontal cortex motor regions in new world monkeys. *Cereb Cortex* 21: 1981–2002, 2011.
- Girard P, Salin PA, Bullier J.** Visual activity in area V2 during reversible inactivation of area 17 in the macaque monkey. *J Neurophysiol* 62: 1287–1302, 1989.
- Girard P, Salin PA, Bullier J.** Visual activity in areas V3a and V3 during reversible inactivation of area V1 in the macaque monkey. *J Neurophysiol* 66: 1493–1503, 1991.
- Girard P, Salin PA, Bullier J.** Response selectivity of neurons in area MT of the macaque monkey during reversible inactivation of area V1. *J Neurophysiol* 67: 1437–1446, 1992.
- Girardin CC, Martin KA.** Cooling in cat visual cortex: stability of orientation selectivity despite changes in responsiveness and spike width. *Neuroscience* 164: 777–787, 2009.
- Godschalk M, Mitz AR, van Duin B, van der Burg H.** Somatotopy of monkey premotor cortex examined with microstimulation. *Neurosci Res* 23: 269–279, 1995.
- Goltz D, Pleger B, Thiel S, Villringer A, Müller MM.** Sustained spatial attention to vibrotactile stimulation in the flutter range: relevant brain regions and their interaction. *PLoS One* 8: e84196, 2013.
- Good PI.** *Resampling Methods: A Practical Guide to Data Analysis*. Boston, MA: Birkhäuser, 2005.
- Gregoriou GG, Borra E, Matelli M, Luppino G.** Architectonic organization of the inferior parietal convexity of the macaque monkey. *J Comp Neurol* 496: 422–451, 2006.
- Hsiao SS, O'Shaughnessy DM, Johnson KO.** Effects of selective attention on spatial form processing in monkey primary and secondary somatosensory cortex. *J Neurophysiol* 70: 444–447, 1993.
- Huang JY, Wang C, Dreher B.** The effects of reversible inactivation of postero-temporal visual cortex on neuronal activities in cat's area 17. *Brain Res* 1138: 111–218, 2007.
- Hyvärinen J.** Regional distribution of functions in parietal association area 7 of the monkey. *Brain Res* 206: 287–303, 1981.
- Hyvärinen J, Poranen A.** Function of the parietal associative area 7 as revealed from cellular discharges in alert monkeys. *Brain* 97: 673–692, 1974.

- Hyvärinen J, Poranen A.** Receptive field integration and submodality convergence in the hand area of the post-central gyrus of the alert monkey. *J Physiol* 283: 539–556, 1978a.
- Hyvärinen J, Poranen A.** Movement-sensitive and direction and orientation-selective cutaneous receptive fields in the hand area of the post-central gyrus in monkeys. *J Physiol* 283: 523–537, 1978b.
- Hyvärinen J, Poranen A, Jokinen Y.** Influence of attentive behavior on neuronal responses to vibration in primary somatosensory cortex of the monkey. *J Neurophysiol* 43: 870–882, 1980.
- Ipata AE, Gee AL, Gottlieb J, Bisley JW, Goldberg ME.** LIP responses to a popout stimulus are reduced if it is overtly ignored. *Nat Neurosci* 9: 1071–1076, 2006.
- Iwamura Y, Iriki A, Tanaka M.** Bilateral hand representation in the post-central somatosensory cortex. *Nature* 369: 554–556, 1994.
- Iwamura Y, Tanaka M.** Rostrocaudal gradients in the neuronal receptive field complexity in the finger region of the alert monkey's postcentral gyrus. *Exp Brain Res* 92: 360–368, 1993.
- Iwamura Y, Tanaka M, Hikosaka O.** Overlapping representation of fingers in the somatosensory cortex (area 2) of the conscious monkey. *Brain Res* 197: 516–520, 1980.
- Iwamura Y, Tanaka M, Iriki A, Taoka M, Toda T.** Processing of tactile and kinesthetic signals from bilateral sides of the body in the postcentral gyrus of awake monkeys. *Behav Brain Res* 135: 185–90, 2002.
- Iwamura Y, Tanaka M, Sakamoto M, Hikosaka O.** Converging patterns of finger representation and complex response properties of neurons in area 1 of the first somatosensory cortex of the conscious monkey. *Exp Brain Res* 51: 327–337, 1983a.
- Iwamura Y, Tanaka M, Sakamoto M, Hikosaka O.** Functional subdivisions representing different finger regions in area 3 of the first somatosensory cortex of the conscious monkey. *Exp Brain Res* 51: 315–326, 1983b.
- Iwamura Y, Tanaka M, Sakamoto M, Hikosaka O.** Vertical neuronal arrays in the postcentral gyrus signaling active touch: a receptive field study in the conscious monkey. *Exp Brain Res* 58: 412–420, 1985a.
- Iwamura Y, Tanaka M, Sakamoto M, Hikosaka O.** Diversity in receptive field properties of vertical neuronal arrays in the crown of the postcentral gyrus of the conscious monkey. *Exp Brain Res* 58: 400–411, 1985b.
- Jansen-Amorim AK, Lima B, Fiorani M, Gattass R.** GABA inactivation of visual area MT modifies the responsiveness and direction selectivity of V2 neurons in Cebus monkeys. *Vis Neurosci* 28: 513–527, 2011.
- Jones SR, Kerr CE, Wan Q, Pritchett DL, Hämäläinen M, Moore CI.** Cued spatial attention drives functionally relevant modulation of the mu rhythm in primary somatosensory cortex. *J Neurosci* 30: 13760–13765, 2010.
- Kaas J, Nelson R, Sur M, Lin C, Merzenich M.** Multiple representations of the body within the primary somatosensory cortex of primates. *Science* 204: 521–523, 1979.
- Kasdon DL, Jacobson S.** The thalamic afferents to the inferior parietal lobule of the rhesus monkey. *J Comp Neurol* 177: 685–706, 1978.
- Krubitzer L, Huffman KJ, Disbrow E, Recanzone G.** Organization of area 3a in macaque monkeys: contributions to the cortical phenotype. *J Comp Neurol* 471: 97–111, 2004.
- Lee S, Kruglikov I, Huang ZJ, Fishell G, Rudy B.** A disinhibitory circuit mediates motor integration in the somatosensory cortex. *Nat Neurosci* 16: 1662–1670, 2013.
- Leinonen L, Hyvärinen J, Nyman G, Linnankoski I.** Functional properties of neurons in lateral part of associative area 7 in awake monkeys. *Exp Brain Res* 34: 299–320, 1979.
- Leinonen L, Nyman G.** II. Functional properties of cells in anterolateral part of area 7 associative face area of awake monkeys. *Exp Brain Res* 34: 321–333, 1979.
- Lewis JW, Van Essen DC.** Corticocortical connections of visual, sensorimotor, and multimodal processing areas in the parietal lobe of the macaque monkey. *J Comp Neurol* 428: 112–137, 2000.
- Lomber SG, Payne BR, Horel JA.** The cryoloop: an adaptable reversible cooling deactivation method for behavioral or electrophysiological assessment of neural function. *J Neurosci Methods* 86: 179–194, 1999.
- London BM, Miller LE.** Responses of somatosensory area 2 neurons to actively and passively generated limb movements. *J Neurophysiol* 109: 1505–1513, 2013.
- Lynch J, Mountcastle V, Talbot W, Yin TC.** Parietal lobe mechanisms for directed visual attention. *J Neurophysiol* 40: 362–389, 1977.
- Meftah EM, Shenasa J, Chapman CE.** Effects of a cross-modal manipulation of attention on somatosensory cortical neuronal responses to tactile stimuli in the monkey. *J Neurophysiol* 88: 3133–3149, 2002.
- Michalski A, Wimborne B, Henry G.** The effect of reversible cooling of cat's primary visual cortex on the responses of area 21a neurons. *J Physiol* 466: 133–156, 1993.
- Mountcastle VB, Lynch JC, Georgopoulos A, Sakata H, Acuna C.** Posterior parietal association cortex of the monkey: command functions for operations within extrapersonal space. *J Neurophysiol* 38: 871–908, 1975.
- Murray GM, Zhang HQ, Kaye AN, Sinnadurai T, Campbell DH, Rowe MJ.** Parallel processing in rabbit first (SI) and second (SII) somatosensory cortical areas: effects of reversible inactivation by cooling of SI on responses in SII. *J Neurophysiol* 68: 703–710, 1992.
- Nassi JJ, Lomber SG, Born RT.** Corticocortical feedback contributes to surround suppression in V1 of the alert primate. *J Neurosci* 33: 8504–8517, 2013.
- Nelissen K, Vanduffel W.** Grasping-related functional magnetic resonance imaging brain responses in the macaque monkey. *J Neurosci* 31: 8220–8229, 2011.
- Nelson RJ, Sur M, Felleman DJ, Kaas JH.** Representations of the body surface in postcentral parietal cortex of *Macaca fascicularis*. *J Comp Neurol* 192: 611–643, 1980.
- Padberg J, Cerkevich C, Engle J, Rajan AT, Recanzone G, Kaas J, Krubitzer L.** Thalamocortical connections of parietal somatosensory cortical fields in macaque monkeys are highly divergent and convergent. *Cereb Cortex* 19: 2038–2064, 2009.
- Padberg J, Disbrow E, Krubitzer L.** The organization and connections of anterior and posterior parietal cortex in titi monkeys: do New World monkeys have an area 2? *Cereb Cortex* 15: 1938–1963, 2005.
- Padberg J, Franca JG, Cooke DF, Soares JG, Rosa MG, Fiorani M, Gattass R, Krubitzer L.** Parallel evolution of cortical areas involved in skilled hand use. *J Neurosci* 27: 10106–10115, 2007.
- Padberg J, Recanzone G, Engle J, Cooke D, Goldring A, Krubitzer L.** Lesions in posterior parietal area 5 in monkeys result in rapid behavioral and cortical plasticity. *J Neurosci* 30: 12918–12935, 2010.
- Pais-Vieira M, Lebedev M, Wiest MC, Nicoletis MA.** Simultaneous top-down modulation of the primary somatosensory cortex and thalamic nuclei during active tactile discrimination. *J Neurosci* 33: 4076–4093, 2013.
- Papadelis C, Eickhoff SB, Zilles K, Ioannides AA.** BA3b and BA1 activate in a serial fashion after median nerve stimulation: direct evidence from combining source analysis of evoked fields and cytoarchitectonic probabilistic maps. *Neuroimage* 54: 60–73, 2011.
- Pei YC, Hsiao SS, Craig JC, Bensmaia SJ.** Shape invariant coding of motion direction in somatosensory cortex. *PLoS Biol* 8: e1000305, 2010.
- Phillips JR, Johnson KO, Hsiao SS.** Spatial pattern representation and transformation in monkey somatosensory cortex. *Proc Natl Acad Sci USA* 85: 1317–1321, 1988.
- Ponce CR, Hunter JN, Pack CC, Lomber SG, Born RT.** Contributions of indirect pathways to visual response properties in macaque middle temporal area MT. *J Neurosci* 31: 3894–3903, 2011.
- Ponce CR, Lomber SG, Born RT.** Integrating motion and depth via parallel pathways. *Nat Neurosci* 11: 216–223, 2008.
- Pons T, Kaas J.** Connections of area 2 of somatosensory cortex with the anterior pulvinar and subdivisions of the ventroposterior complex in macaque monkeys. *J Comp Neurol* 36: 16–36, 1985.
- Pons TP, Garraghty PE, Cusick CG, Kaas JH.** A sequential representation of the occiput, arm, forearm and hand across the rostrocaudal dimension of areas 1, 2 and 5 in macaque monkeys. *Brain Res* 335: 350–353, 1985.
- Pons TP, Garraghty PE, Friedman DP, Mishkin M.** Physiological evidence for serial processing in somatosensory cortex. *Science* 237: 417–420, 1987.
- Pons TP, Kaas JH.** Corticocortical connections of area 2 of somatosensory cortex in macaque monkeys: a correlative anatomical and electrophysiological study. *J Comp Neurol* 248: 313–335, 1986.
- Rozzi S, Calzavara R, Belmalih A, Borra E, Gregoriou GG, Matelli M, Luppino G.** Cortical connections of the inferior parietal cortical convexity of the macaque monkey. *Cereb Cortex* 16: 1389–1417, 2006.
- Rozzi S, Ferrari PF, Bonini L, Rizzolatti G, Fogassi L.** Functional organization of inferior parietal lobule convexity in the macaque monkey: electrophysiological characterization of motor, sensory and mirror responses and their correlation with cytoarchitectonic areas. *Eur J Neurosci* 28: 1569–1588, 2008.
- Sanchez-Panchuelo RM, Besle J, Beckett A, Bowtell R, Schluppeck D, Francis S.** Within-digit functional parcellation of Brodmann areas of the human primary somatosensory cortex using functional magnetic resonance imaging at 7 tesla. *J Neurosci* 32: 15815–15822, 2012.

- Sasaki K, Gemba H.** Compensatory motor function of the somatosensory cortex for the motor cortex temporarily impaired by cooling in the monkey. *Exp Brain Res* 55: 60–68, 1984.
- Schmahmann JD, Pandya DN.** Anatomical investigation of projections from thalamus to posterior parietal cortex in the rhesus monkey: a WGA-HRP and fluorescent tracer study. *J Comp Neurol* 295: 299–326, 1990.
- Seelke AM, Padberg JJ, Disbrow E, Purnell SM, Recanzone G, Krubitzer L.** Topographic maps within Brodmann's area 5 of macaque monkeys. *Cereb Cortex* 22: 1834–1850, 2012.
- Spingath E, Kang HS, Blake DT.** Task-dependent modulation of SI physiological responses to targets and distractors. *J Neurophysiol* 109: 1036–1044, 2013.
- Spingath EY, Kang HS, Plummer T, Blake DT.** Different neuroplasticity for task targets and distractors. *PLoS One* 6: e15342, 2011.
- Sripati AP, Yoshioka T, Denchev P, Hsiao SS, Johnson KO.** Spatiotemporal receptive fields of peripheral afferents and cortical area 3b and 1 neurons in the primate somatosensory system. *J Neurosci* 26: 2101–2114, 2006.
- Sur M.** Receptive fields of neurons in areas 3b and 1 of somatosensory cortex in monkeys. *Brain Res* 198: 465–471, 1980.
- Turman AB, Ferrington DG, Ghosh S, Morley JW, Rowe MJ.** Parallel processing of tactile information in the cerebral cortex of the cat: effect of reversible inactivation of SI on responsiveness of SII neurons. *J Neurophysiol* 67: 411–429, 1992.
- Turman AB, Morley JW, Zhang HQ, Rowe MJ.** Parallel processing of tactile information in cat cerebral cortex: effect of reversible inactivation of SII on SI responses. *J Neurophysiol* 73: 1063–1075, 1995.
- Volgushev M, Kudryashov I, Chistiakova M, Mukovski M, Niesmann J, Eysel UT.** Probability of transmitter release at neocortical synapses at different temperatures. *J Neurophysiol* 92: 212–220, 2004.
- Wacker E, Spitzer B, Lützkendorf R, Bernarding J, Blankenburg F.** Tactile motion and pattern processing assessed with high-field fMRI. *PLoS One* 6: e24860, 2011.
- Wang L, Li X, Hsiao SS, Bodner M, Lenz F, Zhou YD.** Behavioral choice-related neuronal activity in monkey primary somatosensory cortex in a haptic delay task. *J Cogn Neurosci* 24: 1634–1644, 2012.
- Weber JT, Yin TC.** Subcortical projections of the inferior parietal cortex (area 7) in the stump-tailed monkey. *J Comp Neurol* 224: 206–230, 1984.
- Yau JM, Connor CE, Hsiao SS.** Representation of tactile curvature in macaque somatosensory area 2. *J Neurophysiol* 109: 2999–3012, 2013.
- Yeterian EH, Pandya DN.** Corticothalamic connections of the posterior parietal cortex in the rhesus monkey. *J Comp Neurol* 237: 408–426, 1985.
- Zhang H, Murray G.** Parallel processing in cerebral cortex of the marmoset monkey: effect of reversible SI inactivation on tactile responses in SII. *J Neurophysiol* 76: 3633–3655, 1996.
- Zhang H, Zachariah M, Coleman G, Rowe M.** Hierarchical equivalence of somatosensory areas I and II for tactile processing in the cerebral cortex of the marmoset monkey. *J Neurophysiol* 85: 1823–1835, 2001.
- Zhang J, Kriegeskorte N, Carlin JD, Rowe JB.** Choosing the rules: distinct and overlapping frontoparietal representations of task rules for perceptual decisions. *J Neurosci* 33: 11852–11862, 2013.

